

# Icc: an R package to estimate the concordance correlation, Pearson correlation, and accuracy over time

Thiago P Oliveira <sup>Corresp., Equal first author, 1</sup>, Rafael A Moral <sup>Equal first author, 2</sup>, Silvio S Zocchi <sup>3</sup>, Clarice GB Demetrio <sup>3</sup>, John Hinde <sup>1</sup>

<sup>1</sup> School of Mathematics, Statistics and Applied Mathematics, National University of Ireland, Galway, Galway, Co. Galway, Ireland

<sup>2</sup> Department of Mathematics and Statistics, National University of Ireland, Maynooth, Maynooth, Co. Kildare, Ireland

<sup>3</sup> Exact Science, Universidade de São Paulo, Piracicaba, São Paulo, Brazil

Corresponding Author: Thiago P Oliveira

Email address: thiago.paula.oliveira@usp.br

**Background and Objective:** Observational studies and experiments in medicine, pharmacology, and agronomy are often concerned with assessing whether different methods/raters produce similar values over the time when measuring a quantitative variable. This paper aims to describe the statistical package *lcc*, for are, that can be used to estimate the extent of agreement between two (or more) methods over the time, and illustrate the developed methodology using three real examples.

**Methods:** The longitudinal concordance correlation, longitudinal Pearson correlation, and longitudinal accuracy functions can be estimated based on fixed effects and variance components of the mixed-effects regression model. Inference is made through bootstrap confidence intervals and diagnostic can be done via plots, and statistical tests.

**Results:** The main features of the package are estimation and inference about the extent of agreement using numerical and graphical summaries. Moreover, our approach accommodates both balanced and unbalanced experimental designs or observational studies, and allows for different within-group error structures, while allowing for the inclusion of covariates in the linear predictor to control systematic variations in the response. All examples show that our methodology is flexible and can be applied to many different data types.

**Conclusions:** The *lcc* package, available on the CRAN repository, proved to be a useful tool to describe the agreement between two or more methods over time, allowing the detection of changes in the extent of agreement. The inclusion of different structures for the variance-covariance matrices of random effects and residuals makes the package flexible for working with different types of databases.

# 1 lcc: an R package to estimate the 2 concordance correlation, Pearson 3 correlation, and accuracy over time

4 Thiago P. Oliveira<sup>1,2</sup>, Rafael A. Moral<sup>3</sup>, Silvio S. Zocchi<sup>4</sup>, Clarice G. B.  
5 Demétrio<sup>4</sup>, and John Hinde<sup>1</sup>

6 <sup>1</sup>School of Mathematics, Statistics and Applied Mathematics, NUI Galway, Galway  
7 Ireland

8 <sup>2</sup>The Insight Centre for Data Analytics, NUI Galway, Galway Ireland

9 <sup>3</sup>Maynooth University, Maynooth, Co. Kildare, Ireland

10 <sup>4</sup>Luiz de Queiroz College of Agriculture - USP, Piracicaba/SP, Brazil

11 Corresponding author:

12 Thiago Oliveira<sup>1</sup>

13 Email address: thiago.paula.oliveira@usp.br

## 14 ABSTRACT

15 **Background and Objective:** Observational studies and experiments in medicine, pharmacology, and  
16 agronomy are often concerned with assessing whether different methods/raters produce similar values  
17 over the time when measuring a quantitative variable. This paper aims to describe the statistical package  
18 `lcc`, for are, that can be used to estimate the extent of agreement between two (or more) methods over  
19 the time, and illustrate the developed methodology using three real examples.

20  
21 **Methods:** The longitudinal concordance correlation, longitudinal Pearson correlation, and longi-  
22 tudinal accuracy functions can be estimated based on fixed effects and variance components of the  
23 mixed-effects regression model. Inference is made through bootstrap confidence intervals and diagnostic  
24 can be done via plots, and statistical tests.

25  
26 **Results:** The main features of the package are estimation and inference about the extent of  
27 agreement using numerical and graphical summaries. Moreover, our approach accommodates both  
28 balanced and unbalanced experimental designs or observational studies, and allows for different  
29 within-group error structures, while allowing for the inclusion of covariates in the linear predictor to control  
30 systematic variations in the response. All examples show that our methodology is flexible and can be  
31 applied to many different data types.

32  
33 **Conclusions:** The `lcc` package, available on the CRAN repository, proved to be a useful tool  
34 to describe the agreement between two or more methods over time, allowing the detection of changes in  
35 the extent of agreement. The inclusion of different structures for the variance-covariance matrices of  
36 random effects and residuals makes the package flexible for working with different types of databases.

## 37 INTRODUCTION

38 Agreement indices are generally used when the same experimental unit is measured by at least two  
39 methods or observers (King et al., 2007). Measurements of agreement between raters or methods can be  
40 used in any field to explore their interchangeability considering a certain degree of agreement between the  
41 measurements they provide (Barnhart and Williamson, 2001; Chen and Barnhart, 2013). In biomedical  
42 sciences it is often necessary to study the reproducibility of continuous measurements made using specific  
43 diagnostic tools or methods, and that measurements can be taken over the time on the subjects of interest,  
44 such as in the studies of Pandit et al. (2019); Shinar et al. (2019) and Loecher et al. (2019).

45 The concordance correlation coefficient (CCC) introduced by Lin (1989) is a statistic commonly  
46 used to measure the agreement between methods when the response is continuous. Let  $Y_1$  and  $Y_2$  be two

47 random variables with a joint normal distribution

$$\begin{bmatrix} Y_1 \\ Y_2 \end{bmatrix} \sim N_2 \left( \begin{bmatrix} \mu_1 \\ \mu_2 \end{bmatrix}, \boldsymbol{\Sigma} = \begin{bmatrix} \sigma_1^2 & \sigma_{12} \\ \sigma_{12} & \sigma_2^2 \end{bmatrix} \right).$$

48 Here the expected value of the squared difference between  $Y_1$  and  $Y_2$  can be used as an agreement value.  
49 However, it ranges from 0 (perfect agreement) to infinity, which makes its interpretation difficult. Lin  
50 (1989) proposed standardizing this agreement index so that its values lie between  $-1$  and  $+1$ :

$$\rho_{CCC} = 1 - \frac{E[(Y_1 - Y_2)^2]}{\sigma_1^2 + \sigma_2^2 + (\mu_1 - \mu_2)^2} = \frac{2\sigma_{12}}{\sigma_1^2 + \sigma_2^2 + (\mu_1 - \mu_2)^2} = \rho C_b,$$

51 where  $\mu_1 = E(Y_1)$ ,  $\mu_2 = E(Y_2)$ ,  $\sigma_1^2 = \text{Var}(Y_1)$ ,  $\sigma_2^2 = \text{Var}(Y_2)$ , and  $\sigma_{12} = \text{Cov}(Y_1, Y_2)$ . This coefficient  
52 takes the value  $-1$  when there is perfect disagreement, zero when there is no agreement, and  $+1$   
53 when there is perfect agreement. Moreover,  $\rho$ , the Pearson correlation coefficient ( $|\rho| \leq 1$ ), measures  
54 how far each observation deviated from the best-fit line (a precision measure), and  $C_b$ , the accuracy  
55 ( $0 < C_b \leq 1$ ), measures how far the best-fit line deviates from the  $45^\circ$  line through the origin, defined as  
56  $C_b = 2(v + v^{-1} + u^2)^{-1}$ , where  $v = \sigma_1^2/\sigma_2^2$  is a scale shift and  $u = (\mu_1 - \mu_2)/\sqrt{\sigma_1\sigma_2}$  is a location shift  
57 relative to the scale (Lin, 1989). Note that  $C_b = 1$  indicates no deviation from the  $45^\circ$  line.

58 When pairs of samples  $(Y_{i1k}, Y_{i2k})$ , for  $i = 1, 2, \dots, N$  subjects and  $k = 1, 2, \dots, K$  repeated measures,  
59 corresponding to observations on the same subject or experimental unit over time, the use of generalized  
60 multivariate analysis of variance to compute a weighted version of the CCC for repeated measurements is  
61 recommended (Chinchilli et al., 1996). Moreover, this coefficient has also been expanded to assess the  
62 agreement between more than two methods (King and Chinchilli, 2001).

63 When it is necessary to add extra variability sources due to within-subject measurements and/or  
64 other covariates in the model, the CCC can be estimated through the variance components (VC) of a  
65 mixed-effects model (Carrasco et al., 2009). The advantages of the mixed-effects models are that they  
66 give a general approach to analyse repeated measures and unbalanced data; they allow for the inclusion  
67 of different variance-covariance structures for both random effects and sampling errors. The restricted  
68 maximum likelihood (REML) approach can be used to obtain unbiased estimates of the VC.

69 Nevertheless, sometimes the researcher is not interested in reducing the CCC for repeated measure-  
70 ments to a single value, as proposed by Carrasco et al. (2009) and Carrasco et al. (2013), but in describing  
71 the extent of agreement between methods over time. To do this, we can consider a linear or non-linear  
72 function of the time and/or covariates in the model to describe the response variable, as proposed by  
73 Rathnayake and Choudhary (2017) and Oliveira et al. (2018). Here, we present the implementation of  
74 this methodology as an R (R core Team, 2019) package `lcc` (Oliveira et al., 2019), which provides  
75 functions for estimating the longitudinal concordance correlation (LCC) between methods based on  
76 variance components and fixed effects using polynomial mixed-effects models. It also computes estimates  
77 for the longitudinal Pearson correlation (LPC), which measures the precision, and the longitudinal bias  
78 correction factor (LA), which provides an accuracy measure.

79 The `lcc()` function gives fitted values and non-parametric bootstrap confidence intervals for the  
80 LCC, LPC, and LA statistics. Moreover, they can be estimated using different structures for the variance-  
81 covariance matrices of the random effects and different variance functions to model heteroskedasticity of  
82 within-group errors, with the option of using time as a variance covariate.

83 The remainder of the paper is organized as follows: Section introduces the theoretical definition of the  
84 LCC. Section introduces the `lcc()` function input and output, describing in detail the various options as  
85 well the `summary()` and other generic methods. Section briefly discusses model specification, which  
86 is illustrated more extensively in Section using three real data examples. The first and third shows  
87 an application in biomedical science, while the second from food science was the motivation for the  
88 development of the methodology and software and nicely shows the utility of the approach. Finally,  
89 Section presents some final remarks about the `lcc` package.

## 90 MODELS AND COMPUTATIONAL METHODS

91 Suppose a researcher is interested in investigating the extent of agreement between two or more methods,  
92 indexed as  $j = 1, 2, \dots, J$ . Let  $N$  be the number of subjects in the experiment or observational study,

indexed as  $i = 1, 2, \dots, N$ , and suppose that each subject is observed  $n_i$  times (visits) with associated nuisance factors and/or covariates, these could include, for example, the effect of block or group. Let  $y_{ijk}$  be a realization of a random variable  $Y_{ijk}$  measured on the  $i$ -th subject by the  $j$ -th method at time  $t_k$ ,  $k = 1, 2, \dots, n_i$ , with additional subject level (nuisance) covariates  $\mathbf{x}_i$ . Here  $t_k$  assumes values of the time covariate  $t \in \mathcal{T}$ , where  $\mathcal{T}$  denotes the set of measurement times. Hence, the linear mixed-effects model including a polynomial function of time per method, random effects of subject, as well random effects for as subject/time interactions, is given by

$$Y_{ijk} = \boldsymbol{\gamma}^T \mathbf{x}_i + \sum_{h=0}^p \beta_{hj} t_{ik}^h + \sum_{h=0}^q b_{hi} t_{ik}^h + \boldsymbol{\varepsilon}_{ijk}, \quad (1)$$

with  $\mathbf{b}_i \sim \text{MVN}(\mathbf{0}, \mathbf{G})$  and  $\boldsymbol{\varepsilon}_i \sim \text{MVN}(\mathbf{0}, \mathbf{R}_i)$ ,

where  $h = 1, 2, \dots, q, q+1, \dots, p$  is an index identifying the degree of the polynomial, with  $q \leq p$ ;  $Y_{ijk}$  is the response measured on the  $i$ -th subject by the  $j$ -th method at time  $t_{ik}$ ;  $t_{ik}$  represents the time (seconds, minutes, days, etc) at which the  $i$ -th individual was observed;  $\boldsymbol{\gamma}$  is a vector of fixed effect parameters for the subject level covariates;  $\boldsymbol{\beta}_j = [\beta_{0j}, \beta_{1j}, \dots, \beta_{pj}]^T$  is a  $(p+1)$ -dimensional vector of fixed effects for the  $j$ -th method;  $\mathbf{b}_i = [b_{0i}, b_{1i}, \dots, b_{qi}]^T$  is a  $(q+1)$ -dimensional vector of random effects with mean vector  $\mathbf{0}$  and covariance matrix  $\mathbf{G}$ ;  $\boldsymbol{\varepsilon}_i$  is a  $(J \times n_i)$ -dimensional error vector assumed to be independent for different  $i$  and independent of the random effects, with independent entries over  $j$  and  $k$ , with mean vector  $\mathbf{0}$  and diagonal variance matrix  $\mathbf{R}_i$ .

Under model (1), the longitudinal concordance correlation (LCC) function between methods  $j$  and  $j'$ ,  $j \neq j'$ , is given by

$$\rho_{jj'}(t_k) = \frac{\mathbf{t}_k \mathbf{G} \mathbf{t}_k^T}{\mathbf{t}_k \mathbf{G} \mathbf{t}_k^T + \frac{1}{2} \left\{ \sigma_{\boldsymbol{\varepsilon}}^2 [g(t_k, \boldsymbol{\delta}_j) + g(t_k, \boldsymbol{\delta}_{j'})] + S_{jj'}^2(t_k) \right\}} = \rho_{jj'}^{(p)}(t_k) C_{jj'}(t_k) \quad (2)$$

where  $S_{jj'}(t_k) = \mathbf{t}_k (\boldsymbol{\beta}_j - \boldsymbol{\beta}_{j'})$  is the systematic difference between methods  $j$  and  $j'$ ;  $\mathbf{t}_k^T = (t_k^0, t_k^1, \dots, t_k^q)^T$ ;  $g(\cdot)$  is a variance function assumed continuous in  $\boldsymbol{\delta}$ ;  $\boldsymbol{\delta}_j$  is a vector of variance parameters for observations measured by  $j$ -th method or observer. We have that  $\rho_{jj'}^{(p)}(t_k)$  is the longitudinal Pearson correlation (LPC) that measures how far each observation deviated from the best-fit line at a fixed time  $t_k = t$ , given by

$$\rho_{jj'}^{(p)}(t_k) = \frac{\mathbf{t}_k \mathbf{G} \mathbf{t}_k^T}{\sqrt{[\mathbf{t}_k \mathbf{G} \mathbf{t}_k^T + \sigma_{\boldsymbol{\varepsilon}}^2 g(t_k, \boldsymbol{\delta}_j)] [\mathbf{t}_k \mathbf{G} \mathbf{t}_k^T + \sigma_{\boldsymbol{\varepsilon}}^2 g(t_k, \boldsymbol{\delta}_{j'})]}}.$$

$C_{jj'}(t_k)$ , the longitudinal accuracy (LA), measures how far the best-fit line deviates from the  $45^\circ$  line at a fixed time  $t_k = t$ , given by

$$C_{jj'}(t_k) = \frac{2}{v_{jj'}(t_k) + [v_{jj'}(t_k)]^{-1} + u_{jj'}^2(t_k)},$$

where

$$v_{jj'}(t_k) = \sqrt{\frac{\text{Var}(Y_{ijkl})}{\text{Var}(Y_{i'j'kl})}} = \sqrt{\frac{\mathbf{t}_k \mathbf{G} \mathbf{t}_k^T + \sigma_{\boldsymbol{\varepsilon}}^2 g(t_k, \boldsymbol{\delta}_j)}{\mathbf{t}_k \mathbf{G} \mathbf{t}_k^T + \sigma_{\boldsymbol{\varepsilon}}^2 g(t_k, \boldsymbol{\delta}_{j'})}}$$

denotes the scale shift at time  $t_k = t$ , and

$$\begin{aligned} u_{jj'}(t_k) &= \frac{\text{E}(Y_{ijkl}) - \text{E}(Y_{i'j'kl})}{[\text{Var}(Y_{ijkl}) \text{Var}(Y_{i'j'kl})]^{\frac{1}{4}}} \\ &= \frac{\mathbf{t}_k (\boldsymbol{\beta}_j - \boldsymbol{\beta}_{j'})}{\left\{ [\mathbf{t}_k \mathbf{G} \mathbf{t}_k^T + \sigma_{\boldsymbol{\varepsilon}}^2 g(t_k, \boldsymbol{\delta}_j)] [\mathbf{t}_k \mathbf{G} \mathbf{t}_k^T + \sigma_{\boldsymbol{\varepsilon}}^2 g(t_k, \boldsymbol{\delta}_{j'})] \right\}^{\frac{1}{4}}} \end{aligned}$$

denotes the location shift at time  $t_k$  relative to the scale (Lin, 1989; Oliveira et al., 2018). Consequently, when  $\text{Var}(Y_{ijkl}) = \text{Var}(Y_{i'j'kl})$  and  $\text{E}(Y_{ijkl}) = \text{E}(Y_{i'j'kl})$  then  $C_{jj'}(t_k) = 1$  and there is no deviation from the  $45^\circ$  line.

## 121 Estimation and Inference

122 Point estimation and statistical inference for the LCC ( $\rho_{j,j'}(t_k)$ ) has been proposed by Oliveira et al.  
123 (2018). It is estimated by replacing  $\beta$  and the variance components by their respective REML estimates:

$$\hat{\rho}_{j,j'}(t_k) = \frac{\mathbf{t}_k \widehat{\mathbf{G}} \mathbf{t}_k^T}{\mathbf{t}_k \widehat{\mathbf{G}} \mathbf{t}_k^T + \frac{1}{2} \left\{ \widehat{\sigma}_\varepsilon^2 \left[ \widehat{g}(t_k, \widehat{\delta}_j) + \widehat{g}(t_k, \widehat{\delta}_{j'}) \right] + \widehat{S}_{j,j'}^2(t_k) \right\}}.$$

124 Since the variance components are estimated using the REML approach, their estimates are asymp-  
125 totically normally distributed and the bias is smaller when compared to the maximum likelihood (ML)  
126 approach. Moreover, Oliveira et al. (2018) showed a satisfactory performance of the LCC even in settings  
127 with severe imbalance and only a small number of subjects ( $N = 20$ ).

128 A confidence interval (CI) for  $\rho_{j,j'}(t_k)$  can be constructed using a nonparametric bootstrap based on  $M$   
129 (e.g. 5000) bootstrap samples with either the percentile method (recommended for  $N \leq 30$ ) or, otherwise,  
130 a normal approximation confidence interval, as described by Oliveira et al. (2018).

When we use a normal approximation for the CI, the Fisher Z-transformation given by

$$\rho_{j,j'}^*(t_k) = \frac{1}{2} \ln \left[ \frac{1 + \rho_{j,j'}(t_k)}{1 - \rho_{j,j'}(t_k)} \right]$$

should be used with the normal approximation made to the empirical distribution of  $\rho_{j,j'}^*(t_k)$  (Lin, 1989).  
Consequently, the confidence limits can be estimated using the bootstrap estimator of  $\rho_{j,j'}^*(t_k)$  for a fixed  
time  $t_k = t$  given by

$$\widehat{\rho}_{j,j'}^*(t_k = t) = \frac{1}{2M} \sum_{m=1}^M \ln \left[ \frac{1 + \widehat{\rho}_{j,j'}^{(m)}(t)}{1 - \widehat{\rho}_{j,j'}^{(m)}(t)} \right], \quad m = 1, 2, \dots, M,$$

where  $\{\widehat{\rho}_{j,j'}^{(m)}\}$  are the estimates from the  $M$  bootstrap samples. The standard deviation of the bootstrap  
distribution of  $\widehat{\rho}_{j,j'}^*(t_k)$  for a fixed time  $t_k = t$  given by

$$\widehat{SE}_{j,j'}^*(t_k = t) = \sqrt{\frac{1}{M-1} \sum_{m=1}^M \left[ \frac{1}{2} \ln \left( \frac{1 + \widehat{\rho}_{j,j'}^{(m)}(t)}{1 - \widehat{\rho}_{j,j'}^{(m)}(t)} \right) - \widehat{\rho}_{j,j'}^*(t) \right]^2}.$$

131 Thus, an approximate bootstrap confidence interval of level  $(1 - \alpha)$  for  $\rho_{j,j'}$  is  $[LB, UB]$ , where

$$LB = \frac{\exp \left\{ 2 \left[ \widehat{\rho}_{j,j'}^*(t_k = t) - z_{(1-\frac{\alpha}{2})} \widehat{SE}_{j,j'}^*(t_k = t) \right] \right\} - 1}{\exp \left\{ 2 \left[ \widehat{\rho}_{j,j'}^*(t_k = t) - z_{(1-\frac{\alpha}{2})} \widehat{SE}_{j,j'}^*(t_k = t) \right] \right\} + 1}$$

132 and

$$UB = \frac{\exp \left\{ 2 \left[ \widehat{\rho}_{j,j'}^*(t_k = t) - z_{\frac{\alpha}{2}} \widehat{SE}_{j,j'}^*(t_k = t) \right] \right\} - 1}{\exp \left\{ 2 \left[ \widehat{\rho}_{j,j'}^*(t_k = t) - z_{\frac{\alpha}{2}} \widehat{SE}_{j,j'}^*(t_k = t) \right] \right\} + 1},$$

133 where  $z_{\frac{\alpha}{2}}$  and  $z_{(1-\frac{\alpha}{2})}$  denote the  $\frac{\alpha}{2}$  and  $(1 - \frac{\alpha}{2})$  percentiles of the standard normal distribution.

On the other hand, the CI based on the percentile method uses the percentiles of the bootstrap  
distribution of  $\widehat{\rho}_{j,j'}^*(t_k = t)$  directly and is given by

$$\left( \widehat{\rho}_{(j,j')(\alpha/2)}^*(t_k = t), \widehat{\rho}_{(j,j')(1-\alpha/2)}^*(t_k = t) \right) \approx \left( \widehat{\rho}_{(j,j')(\alpha/2)}^{(m)}(t_k = t), \widehat{\rho}_{(j,j')(1-\alpha/2)}^{(m)}(t_k = t) \right),$$

134 where  $\widehat{\rho}_{(j,j')(\alpha/2)}^{(m)}(t_k = t)$  and  $\widehat{\rho}_{(j,j')(1-\alpha/2)}^{(m)}(t_k = t)$  are the  $(100 \times \frac{\alpha}{2})$ -th and  $(100 \times 1 - \frac{\alpha}{2})$ -th empirical  
135 percentiles of the  $\widehat{\rho}_{j,j'}^{(m)}(t_k = t)$  values,  $m = 1, 2, \dots, M$ . If the bootstrap distribution of  $\rho_{j,j'}^*(t_k = t)$  is  
136 approximately normal, then both proposed methods will give very similar confidence intervals as  $N$   
137 increases.

Inference for  $C_{j,j'}(t_k)$  can be performed in a similar way as to that presented for the LCC. Since  $C_{(j,j')(1-\alpha/2)}(t_k = t)$  belongs to the interval  $[0, 1]$ , we suggest the use the arc-sine transformation

$$C_{(j,j')(1-\alpha/2)}^*(t_k = t) = \sin^{-1} \sqrt{C_{j,j'}(t_k)}$$

instead of the Fisher Z-transformation, nor logistic transformation (used by Oliveira et al. (2018)) to approximate the distribution of  $C_{(j,j')(1-\alpha/2)}(t_k = t)$  by a normal distribution. Thus, the confidence limits can be estimated using the bootstrap estimator of  $C_{j,j'}^*(t_k)$  for a fixed time  $t_k = t$  given by

$$\widehat{C}_{j,j'}^*(t_k = t) = \frac{1}{M} \sum_{m=1}^M \sin^{-1} \sqrt{\widehat{C}_{j,j'}^{(m)}(t)}, \quad m = 1, 2, \dots, M,$$

and standard deviation of the bootstrap distribution of  $\widehat{C}_{j,j'}^*(t_k)$  for a fixed time  $t_k = t$  is given by

$$\widehat{SE}_{C_{j,j'}^*}(t_k = t) = \sqrt{\frac{1}{M-1} \sum_{m=1}^M \left[ \sin^{-1} \sqrt{\widehat{C}_{j,j'}^{(m)}(t)} - \widehat{C}_{j,j'}^*(t) \right]^2}.$$

Therefore, an approximate bootstrap confidence interval of level  $(1 - \alpha)$  for  $\widehat{C}_{j,j'}$  is  $[LB_C, UB_C]$ , where

$$LB_C = \text{sign} \left[ \widehat{C}_{j,j'}^*(t_k = t) - z_{(1-\frac{\alpha}{2})} \widehat{SE}_{C_{j,j'}^*}(t_k = t) \right] \left\{ \sin \left[ \widehat{C}_{j,j'}^*(t_k = t) - z_{(1-\frac{\alpha}{2})} \widehat{SE}_{C_{j,j'}^*}(t_k = t) \right] \right\}^2$$

and

$$UB_C = \text{sign} \left[ \widehat{C}_{j,j'}^*(t_k = t) - z_{\frac{\alpha}{2}} \widehat{SE}_{C_{j,j'}^*}(t_k = t) \right] \left\{ \sin \left[ \widehat{C}_{j,j'}^*(t_k = t) - z_{\frac{\alpha}{2}} \widehat{SE}_{C_{j,j'}^*}(t_k = t) \right] \right\}^2,$$

where  $z_{\frac{\alpha}{2}}$  and  $z_{(1-\frac{\alpha}{2})}$  denote the  $(\frac{\alpha}{2})$  and  $(1 - \frac{\alpha}{2})$  quantiles of the standard normal distribution. Bootstrap percentile intervals are calculated in the obvious way from the bootstrap values  $\widehat{C}_{j,j'}^{(m)}(t)$ ,  $m = 1, 2, \dots, M$ .

## OVERVIEW OF THE PACKAGE LCC AND R SYNTAX

This section provides some details on the implementation of the function `lcc` and explains its technical arguments, whose default settings were carefully chosen. The package is freely available for download from the CRAN website <https://CRAN.R-project.org/package=lcc>, and installation can be performed using

```
R> install.packages("lcc")
R> library(lcc)
```

The `lcc` package has 21 arguments that are briefly summarised in Table 1.

**Table 1.** Input arguments for LCC package

Argument	Type	Description	Default	Required
<code>data</code>	<code>data.frame</code>	Specifies the input dataset		Yes
<code>resp</code>	Character string	Name of the response variable		Yes
<code>subject</code>	Character string	Name of the subject variable		Yes
<code>method</code>	Character string	Name of the method variable		Yes
<code>time</code>	Character string	Name of the time variable		Yes

Continued on next page

**Table 1 – continued from previous page**

Argument	Type	Description	Default	Required
<code>interaction</code>	Logical	an option to estimate the interaction effects between method and time. If <code>TRUE</code> the interaction effects are estimated. If <code>FALSE</code> only the main effects of time and method are estimated	<code>TRUE</code>	No
<code>qf</code>	Numeric	An integer specifying the degree of the polynomial time trends, usually 1, 2 or 3 (0 is not allowed).	1	No
<code>qr</code>	Numeric	An integer specifying terms having random effects to account for subject-to-subject variation, such that $qr \leq qf$ , and $qr=0$ means there is just a random intercept.	0	No
<code>covar</code>	Character vector	Names of the covariates (factors and/or variables) to include in the model as fixed effects, e.g. <code>block</code> , <code>group</code> , etc.	<code>NULL</code>	No
<code>gs</code>	Character string	Name of method level which represents the gold-standard.	<code>first level</code>	No
<code>pdmat</code>	Function	Standard classes of positive-definite matrix structures available in the <code>nlme</code> package.	<code>pdSymm</code>	No
<code>var.class</code>	Function	Standard classes of variance function structures used to model the variance structure of within-group errors using covariates.	<code>NULL</code>	No
<code>weights.form</code>	Formula	An one-sided formula specifying a variance covariate and, optionally, a grouping factor for the variance parameters in the <code>var.class</code> . If <code>var.class = varIdent</code> , the form <code>"method"</code> , (or <code>~ 1   method</code> ), or <code>"time.ident"</code> ( <code>~ 1   time</code> ), must be used. If <code>var.class = varExp</code> , the form <code>"time"</code> ( <code>~ time</code> ), or <code>"both"</code> ( <code>~ time   method</code> ), must be used.	<code>NULL</code>	No <sup>1</sup>
<code>time.lcc</code>	List	Regular sequence for time variable merged with specific or experimental time values used for LCC, LPC, and LA predictions.	<code>NULL</code>	No
<code>ci</code>	Logical	An optional non-parametric bootstrap confidence interval for the LCC, LPC and LA statistics. If <code>TRUE</code> confidence intervals are calculated and printed in the output.	<code>FALSE</code>	No

Continued on next page

<sup>1</sup>Required when `var.class` is specified.

Table 1 – continued from previous page

Argument	Type	Description	Default	Required
percentileMet	Logical	an optional method for calculating the non-parametric bootstrap intervals. If FALSE the normal approximation method is used. If TRUE the percentile method is used.	FALSE	No <sup>2</sup>
alpha	Numeric	Confidence level for the CI.	0.05	No <sup>2</sup>
nboot	Numeric	An integer specifying the number of bootstrap samples.	5000	No <sup>2</sup>
show.warnings	Logical	an optional argument that shows the number of convergence errors in the bootstrap samples. If TRUE shows in which bootstrap samples the errors occurred. If FALSE shows the total number of convergence errors.	FALSE	No
components	Logical	An option to estimate the LPC and LA statistics. If TRUE the estimates and confidence intervals for LPC and LA are printed in the output. If FALSE provides estimates and confidence intervals only for the LCC statistic.	FALSE	No
REML	Logical	The estimation method. If TRUE the model is fit by maximizing the restricted log-likelihood. If FALSE full maximum likelihood is used.	TRUE	No
lme.control	List	A list of control values passed to the estimation algorithm to replace the default values of the function <code>lmeControl</code> available in the <code>nlme</code> package.	empty list	No

150 We present a more detailed description of some arguments below:

- 151 1. `data`: must be a data frame containing the following variables: response, subject identification,  
152 method, and time;
- 153 2. `method`: name of the method variable in the dataset. The `lcc` package recognizes the first level  
154 of the variable associated with this argument as the gold-standard method, and then compares it  
155 with all other levels;
- 156 3. `qr`: when we specify `qr = 0` a random intercept is included in the polynomial model while `qr`  
157 `= 1` specifies random intercepts and slopes. If `qr = qf = q`, with  $q \geq 1$ , all polynomial terms  
158 are specified to have random effects at the individual level.
- 159 4. `time.lcc`: a named list with values for arguments `time`, `from`, `to`, and `n` used in the `time.lcc()`  
160 function to generate a regular sequence merged with specific or experimental time values of the  
161 time variable used for LCC, LPC and LA predictions. Argument `time` is a vector of specific or  
162 experimental time values of a given length, where the experimental time values are used as default;  
163 `from` and `to` are used to define, respectively, the starting and end values of the time variable, and  
164 `n` is used to define the desired length of the sequence. We recommend a grid  $\mathbf{t} = (t_1, t_2, \dots, t_{n^*})^T$  of  
165  $n^*$  points in  $\mathcal{T}$  to construct the agreement curve and confidence intervals. In practice,  $n^*$  between  
166 30 and 50 is generally adequate. Example:

<sup>2</sup>It can only be specified when `ci = TRUE`

```

167 R> Time <- seq(0,20,1)
168 R> str(tk <- time_lcc(time=Time, from=min(Time), to=max(Time),
169 + n=30))
170 num [1:49] 0 0.69 1 1.38 2 ...

```

- 171 5. `pdmat`: the `lcc` package provides six standard classes of positive-definite matrix structures that  
 172 can be included in the model to estimate the LCC, LPC and LA statistics. Available standard  
 173 classes are `pdSymm`, `pdLogChol`, `pdDiag`, `pdIdent`, `pdCompSymm`, and `pdNatural`. More  
 174 information about these classes are available in Pinheiro and Bates (2000).
- 175 6. `var.class`: a class of variance functions that are used to model the variance structure of within-  
 176 group errors using covariates (Pinheiro and Bates, 2000). We generalize this class as

$$\text{Var}(\epsilon_{ijk}) = \sigma_{\epsilon}^2 g(t_k, \boldsymbol{\delta}), \quad (3)$$

177 where  $g(\cdot)$  is the variance function assumed continuous in  $\boldsymbol{\delta}$ ;  $t_k$  is the time covariate and  $\boldsymbol{\delta}$  is a  
 178 vector of variance parameters. The `lcc` package provides two different standard variance functions  
 179 classes that are included in the `nlme` library (Pinheiro et al., 2017).

180 The first one is the `varIdent` class that represent a variance model with different variances for  
 181 each level of a stratification variable  $s$ ,  $s = 1, 2, \dots, S$ , given by

$$\text{Var}(\epsilon_{ijk}) = \sigma_{\epsilon}^2 \delta_{s_{ijk}}^2.$$

182 As we have  $S+1$  parameters to represent  $S$  variances, we need to add the restriction  $\delta_1 = 1$ , and  
 183 consequently  $\delta_{s^*} = \delta_{s^*} / \delta_1$ ,  $s^* = 2, 3, \dots, S$  and  $\delta_{s^*} > 0$ . Here each level of method/observer or time  
 184 represents a stratum of a homogeneous subgroup.

185 The second variance function is an exponential function of the variance covariate, the `varExp`  
 186 class, represented as

$$\text{Var}(\epsilon_{ijk}) = \sigma_{\epsilon}^2 \exp(2\delta_{s_{ijk}} t_k)$$

187 where  $\delta_{s_{ijk}}$  is unrestricted, so the variance model (4) allows  $\text{Var}(\epsilon_{ijk})$  to increase or decrease over  
 188 time.

- 189 7. `weights.form`: a `varFunc` class object, representing a constructor to the `form` argument in  
 190 the `nlme` library. The `weights.form` argument is based on a one-sided formula specifying a  
 191 variance covariate and, optionally, a grouping factor for the variance parameters. Moreover, this  
 192 argument must be specified only when `var.class` is specified as well.

193 The first class `varIdent` represents a variance model with different variances for each level of  
 194 the grouping factor and has two options of `weights.form` in the `lcc` package:

- 195 (a) "method": specifies a variance model with different variances for each level of factor  
 196 method/observer and is given by

$$\text{Var}(\epsilon_{ijk}) = \sigma_{\epsilon}^2 \delta_{\text{method}_j}^2, \quad j = 1, 2, \dots, J,$$

197 where  $g(\text{method}_j, \delta_j) = \delta_{\text{method}_j}^2$  is the variance function, and  $\delta_{\text{method}_j}$  is the variance param-  
 198 eter for observations measured by the  $j$ th method. The `form` argument in the `varFunc` is  
 199 `form = ~ 1|method`;

- 200 (b) "time.ident": specifies a variance model with different variances for each level of  
 201 stratification in the time variable and is given by

$$\text{Var}(\epsilon_{ijk}) = \sigma_{\epsilon}^2 \delta_{t_k}^2, \quad k = 1, 2, \dots, K,$$

202 where  $g(t_k, \delta_k) = \delta_k^2$  is the variance function, and  $\delta_k$  is the variance parameter for obser-  
 203 vations measured at time  $t_k = t$ , with  $t \in [t_0, t_K]$  and  $t_0 \geq 0$ . The `form` argument in the  
 204 `varFunc` class is `form = ~ 1|time`.

205 The class `varExp` represents a variance model whose variance function  $g(\cdot)$  is an exponential  
 206 function of the variance covariate. This class has also two options of `weights.form` in the `lcc`  
 207 package:

208 (a) `"time"`: specifies a variance model given by

$$\text{Var}(\varepsilon_{ijk}) = \sigma_{\varepsilon}^2 \exp(2\delta t_k),$$

209 where the variance function  $g(t_k, \delta) = \exp(2\delta t_k)$  is an exponential function of the time  $t_k = t$ ;  
 210 and  $\delta$  is the variance parameter. The `form` argument in the `varFunc` class is `form = ~`  
 211 `time`;

212 (b) `"both"`: specify a variance model for each level of the factor method given by

$$\text{Var}(\varepsilon_{ijk}) = \sigma_{\varepsilon}^2 \exp\left(2\delta_{\text{method}_j} t_k\right), \quad j = 1, 2, \dots, J,$$

213 where the variance function  $g(t_k, \text{method}_j, \delta) = \exp\left(2\delta_{\text{method}_j} t_k\right)$  is an exponential function  
 214 of the time  $t_k = t$  for each level of method; and  $\delta_{\text{method}_j}$  is the variance parameter for the  $j$ th  
 215 level of method. The `form` argument in the `varFunc` class is `form = ~ time|method`;

216 The `lcc` package uses the REML method as default because it is less biased, less sensitive to outliers,  
 217 and deals more effectively with high correlations when compared to standard ML estimation (Harville,  
 218 1977; Giesbrecht and Burns, 1985). However, we offer the user the possibility to change the estimation  
 219 method to ML because this approach should be used when comparing models with nested fixed effects but  
 220 with the same random effects structure. Furthermore, the package depends on the `nlme` (Pinheiro et al.,  
 221 2017), and `ggplot2` (Wickham, 2009) packages, and imports some functions from packages `gdata`  
 222 (Warnes et al., 2017), `gridExtra` (Aguie and Antonov, 2017), and `hnp` (Moral et al., 2017).

### 223 Generic functions and outputs

224 A typical call of the `lcc` function is similar to a call to `lme` as the LCC estimation is based on a  
 225 mixed-effects regression model. Several variations in the specifications of linear mixed-effects models to  
 226 estimate the LCC are possible, and we can query the fitted `lcc` object through different generic functions.  
 227 Table 2 gives details of a set of S3 generic extractor functions for objects of class `lcc`.

228 The output of the `summary()` function includes the values of Akaike Information Criterion (AIC)  
 229 (Akaike, 1974), the Bayesian Information Criterion (BIC) (Schwarz, 1978), log-likelihood value, and a  
 230 goodness of fit measurement `gof`, which is calculated using the concordance correlation coefficient (Lin,  
 231 1989) between fitted values extracted from the mixed-effects model and observed values. This measure  
 232 can be used, with care, to describe the overall agreement between observed and fitted values, where a  
 233 value equal to  $-1$  represents a perfect disagreement between them, zero represents no agreement, and  
 234  $+1$  perfect agreement. Clearly, a high model performance is related with a high positive value of `gof`  
 235 (generally between 0.8-1).

236 The fitted curves of LCC, LPC, or LA values versus the time covariate, as well as their boot-  
 237 strap confidence intervals, can be visualised through the `lccPlot()` function, which is specified as  
 238 `lccPlot(obj, type, control)`, where `obj` is an object of class `lcc`; `type` specifies required  
 239 output that could be `type="lcc"` for the LCC, the default, `type="lpc"` for the LPC, or `type="la"`  
 240 for the LA statistics; and `control` is a list of control values or character strings returned by the  
 241 `plotControl()` function used to modify the plot structure. This function uses the `ggplot2` package  
 242 internally to build the final plot, where predicted values are joined by lines, sampled observations are  
 243 represented by circles, and confidence intervals by a ribbon (grey as default) defined by its lower and  
 244 upper bounds.

### 245 SPECIFYING MODELS IN THE `LCC()` FUNCTION

246 In the `lcc` package, to describe the LCC we need to specify the subject, response, method and time  
 247 variables, a polynomial mixed-effect model, and the data. These arguments are specified through an

**Table 2.** Generic functions for use with objects of class `lcc`

Function	Description
<code>print()</code>	a simple printed display
<code>summary()</code>	returns an object of class <code>summary.lcc</code> containing the relevant summary statistics (which has a <code>print()</code> method). If <code>type = "lcc"</code> it provides information about $\rho_{jj'}(t_k)$ , and if <code>components = TRUE</code> in the <code>lcc()</code> function, also provides information about $\rho_{jj'}^{(p)}(t_k)$ , and $C_{jj'}(t_k)$ . If <code>type = "model"</code> it provides additional information about the linear mixed-effects fit. The default is <code>type = "model"</code> .
<code>anova()</code>	Summarise and compare likelihoods of fitted models from <code>lcc</code> objects
<code>coef()</code>	The fixed effects estimated and corresponding random effects estimates are obtained at subject levels less or equal to $N$ . The resulting estimates are returned as a data frame, with rows corresponding to subject levels and columns as coefficients.
<code>fitted()</code>	Fitted values for $\hat{\rho}_{jj'}(t_k)$ , $\hat{\rho}_{jj'}^{(p)}(t_k)$ , or $\hat{C}_{jj'}(t_k)$ . The output depends on the argument <code>type</code> , where <code>type = "lcc"</code> (the default), <code>type = "lpc"</code> , or <code>type = "la"</code> gives output for $\hat{\rho}_{jj'}(t_k)$ , $\hat{\rho}_{jj'}^{(p)}(t_k)$ , or $\hat{C}_{jj'}(t_k)$ , respectively.
<code>getVarCov()</code>	Returns the variance components estimates.
<code>residuals()</code>	Extract residuals (response, Pearson, and normalized), defaulting to Pearson residuals
<code>ranef()</code>	Extract the estimated random effects.
<code>vcov()</code>	Returns the variance-covariance matrix of the fixed effects.
<code>AIC()</code>	Compute the Akaike criterion
<code>BIC()</code>	Compute the Bayesian criterion
<code>logLik()</code>	Extract the log-likelihood
<code>plot()</code>	A series of six built-in diagnostic plots to evaluate the assumptions underlying the linear mixed-effects regression model. Comprises: a plot of conditional residuals against fitted values; plot of conditional residuals over time; box-plot of residuals given subject; observed against fitted values; normal Q-Q plot with simulation envelopes for the conditional errors; and normal Q-Q plot with simulation envelopes for the random effects are provided.

248 easy-to-use syntax. Consider a first degree polynomial model with random intercepts for a continuous  
 249 dependent variable  $y$  observed on  $N$  subjects ( $i = 1, 2, \dots, N$ ) using  $J$  methods at times  $t_k$  ( $k = 1, 2, \dots, n_i$ ).  
 250 Such model can be written as

$$Y_{ijk} = \beta_{0j} + b_{0i} + \beta_{1j}t_k + \varepsilon_{ijk}, \text{ with} \\ b_{0i} \sim N(0, \sigma_{b_0}^2) \text{ and } \varepsilon_{ijk} \sim N(0, \sigma_\varepsilon^2)$$

251 Thus, the LCC based on fixed effects and variance components at time  $t_k$  is given by

$$\rho_{jj'}(t_k) = \frac{\sigma_{b_0}^2}{\sigma_{b_0}^2 + \sigma_\varepsilon^2 + \frac{1}{2}[\beta_{01} - \beta_{02} + (\beta_{11} - \beta_{12})t_k]^2}$$

252 and the syntax to specify this model in the `lcc()` function is

```
253 R> library(lcc)
254 R> data(simulated_hue_block)
255 R> m1 <- lcc(data = simulated_hue_block, subject = "Fruit",
256 +           resp = "Hue", method = "Method", time = "Time",
257 +           qf = 1, qr = 0)
```

258 where `qf = 1` represents the polynomial degree for the fixed effects, and `qr = 0` specifies a random  
 259 intercepts model. Here, the names of the columns in the dataframe `data` are supplied as strings to the  
 260 arguments of the `lcc()` function.

261 Suppose now that the experimental design in the previous example was a randomized complete block  
 262 design. Then, the fixed effect of blocks can be included in that model by specifying the `covar` argument,  
 263 i.e.

```
264 R> m2 <- update(m1, covar = "Block")
```

265 If we suppose different variances for each level of the method factor, the corresponding model would  
 266 include a variance function such as  $g(\delta_j) = \sigma_\epsilon^2 \delta_j^2$ , and the syntax would then be

```
267 R> m3 <- update(m2, var.class = varIdent, weights.form = "method",  

  268 + lme.control = list(opt="optim"))
```

269 To visualize the summary and graphical output of model `m3` we call `summary(m3)` and `lccPlot(m3)`,  
 270 respectively.

271 Many other possible models can be built to estimate the LCC through the function `lcc()` options,  
 272 see Section . Model selection can be performed using likelihood-ratio tests for nested models; or using  
 273 the AIC or BIC criteria, e.g.

```
274 R> AIC(m2, m3); BIC(m2, m3); anova(m2, m3)
```

## 275 EXAMPLES

276 We will now use three example datasets, drawn from Lloyd et al. (1998), Martin et al. (2002) and Oliveira  
 277 et al. (2018), to illustrate the implemented functions in the following sections of this paper. The first  
 278 dataset is an observational study of a cohort of 82 adolescent females to assess the percentage body fat  
 279 and the aim is to determine the agreement profile between measurements made over time using a skinfold  
 280 caliper and dual-energy X-ray absorptiometry. The second is a canonical example from agriculture and  
 281 was the motivation for the original development of these methods; here the goal is to investigate if a  
 282 colorimeter can compete with a digital scanner in measuring the peel hue of papayas over time. The  
 283 final example is again related to medicine and the goal here is to verify the agreement between cortisol  
 284 concentration measured on patients every hour and every two hours.

### 285 Percentage body fat dataset

286 These data came from a longitudinal observational study conducted as part of the Penn State Young  
 287 Women's Health Study (Lloyd et al., 1998). Percentage body fat was measured using skinfold calipers and  
 288 dual-energy X-ray absorptiometry (DEXA) on a cohort of 82 adolescent white females attending public  
 289 schools in Pennsylvania. The initial visit occurred at age 12 (baseline) and subsequent visits occurred  
 290 every six months, in which one skinfold caliper and one DEXA measurement were taken to assess the  
 291 percentage of body fat. As the skinfold measurement is the most frequently used method for laboratory  
 292 and field studies, the objective was to determine the agreement profile between the skinfold caliper  
 293 and DEXA measurements. Figure 1 shows that the agreement between skinfold and DEXA apparently  
 decreases over the visits. King et al. (2007) explained that this phenomenon may occur because the

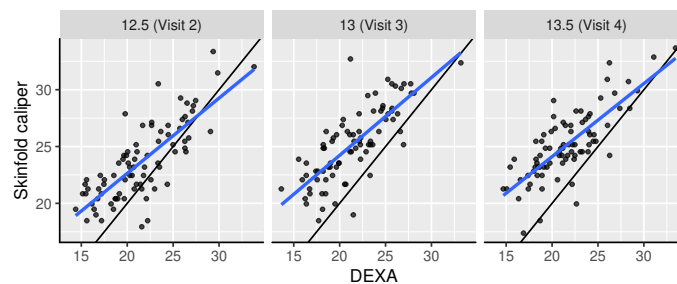


**Figure 1.** Scatter plot of body fat data, where the panels represent visits, the blue line is the best fit line, and the black line is the line of equality.

294

295 skinfold method is only capable of detecting subcutaneous fat, while DEXA detects subcutaneous, breast,  
 296 lower body and visceral fat. Moreover, female adolescents may have a considerable fat increase in breast,  
 297 lower body and/or visceral fat over this age range (King et al., 2007). Consequently, this reinforces the  
 298 interest in estimating the agreement profile between these methods for the body fat measurements over  
 299 ages ranging from 12.5 to 13.5 years old, rather than summarizing it in a single coefficient as proposed  
 300 by King et al. (2007). Hence, we created a new variable called `TIME` given by  $12 \times (\text{age} - 12)$ , which  
 301 represents the time in months after the first visit (baseline).

Now let  $y_{ijk}$  be the measurement taken on the  $i$ -th individual, by the  $j$ -th method at the  $k$ -th visit. We then fit a random intercepts and slopes linear regression model, given by

$$y_{ijk} = \beta_{0j} + b_{0i} + (\beta_{1j} + b_{1i})t_k + \varepsilon_{ijk} \quad (4)$$

$$\mathbf{b} = [b_{0i}, b_{1i}]^T \sim N_2(\mathbf{0}, \mathbf{G}) \quad \text{and} \quad \varepsilon_{ijk} \sim N(0, \sigma_\varepsilon^2),$$

302 where  $\text{vech}(\mathbf{G}) = [\sigma_{b_0}^2, \sigma_{b_{01}}, \sigma_{b_1}^2]^T$  ( $\text{vech}(\cdot)$  is the half-vectorization of a symmetric matrix  $\mathbf{G}$  formed  
 303 from only the lower triangular part). Using model (4), we estimate the LCC, LPC and LA statistics as well  
 304 as their 95% bootstrap confidence intervals based on 10,000 pseudo-samples using the `lcc()` function:

```
305 R> data(bfat, package = "cccrm")
306 R> library(dplyr)
307 R> bfat <- bfat %>%
308 +   mutate(VISITNO = replace(VISITNO, VISITNO == 2, 12.5)) %>%
309 +   mutate(VISITNO = replace(VISITNO, VISITNO == 3, 13)) %>%
310 +   mutate(VISITNO = replace(VISITNO, VISITNO == 4, 13.5)) %>%
311 +   mutate(SUBJECT = factor(SUBJECT)) %>%
312 +   mutate(MET = factor(MET, labels = c("1 hour", "2 hours")))
313 R> bfat$TIME <- 12 * (bfat$VISITNO - 12)
314 R> m.bfat.1 <- lcc(data = bfat, subject = "SUBJECT", resp = "BF",
315 +   method = "MET", time = "TIME", qf = 1, qr = 1,
316 +   components = TRUE, ci = TRUE, nboot = 10000)
317 Convergence error in 951 out of 10000 bootstrap samples.
```

318 The output of model `m.bfat.1` indicates that in 951 (9.51%) of the pseudo-samples, the likelihood  
 319 maximization algorithm failed to converge, where most of these failures were a consequence of specific  
 320 bootstrap sample patterns. An alternative procedure to decrease the percentage of convergence failures  
 321 is by increasing the iteration limit and/or changing the optimization method from `nlminb` to `optim`.  
 322 In the `lcc()` function, the user can include a list of optimisation control additional arguments in the  
 323 `lme.control()` function:

```
324 R> m.bfat.2 <- update(m.bfat.1, lme.control = list(opt = "optim"))
325 Convergence error in 72 out of 10000 bootstrap samples.
```

326 The output of `m.bfat.2` shows a lower number of failures (0.72%) compared with the previous  
 327 approach. We proceed to examine the bootstrap confidence intervals computed for the LCC, LPC and LA:

```
328 R> summary(m.bfat.2, type = "lcc")
329 Longitudinal concordance correlation model fit by REML
330 AIC      BIC      logLik
331 2182.068  2215.59  -1083.034
332
333 gof: 0.9201
334
335 Lower and upper bound of % bootstrap confidence interval
336 Number of bootstrap samples:
337
338 DEXA vs. skinfold
339 $LCC
340   Time      LCC      Lower      Upper
```

```

341 1     6   0.6653516   0.5687779   0.7395459
342 2    12   0.5589258   0.4516374   0.6442955
343 3    18   0.4588008   0.3353932   0.5599172

```

```
344
```

```
345 $LPC
```

```

346   Time      LPC      Lower      Upper
347 1     6   0.8065578   0.7415331   0.8558988
348 2    12   0.7826493   0.7092871   0.8378992
349 3    18   0.7620551   0.6676806   0.8300397

```

```
350
```

```
351 $LA
```

```

352   Time      LA      Lower      Upper
353 1     6   0.8249273   0.7431156   0.8898124
354 2    12   0.7141458   0.6201347   0.7923521
355 3    18   0.6020573   0.4934167   0.6961643

```

356 We may then plot the LCC, LPC, and LA with their respective confidence intervals by executing

```

357 R> lccPlot(m.bfat.2)
358 R> lccPlot(m.bfat.2, type = "lpc")
359 R> lccPlot(m.bfat.2, type = "la")

```

360 The estimates of LCC, LPC and LA, their confidence intervals, and figures indicate that the agreement  
 361 and accuracy profiles between the skinfold caliper and DEXA measurements decrease over time, while  
 362 the precision profile, represented by LPC, remains constant (Figure 2). Therefore, a first conclusion is  
 363 that the agreement profile decreases over time because the accuracy is decreasing.

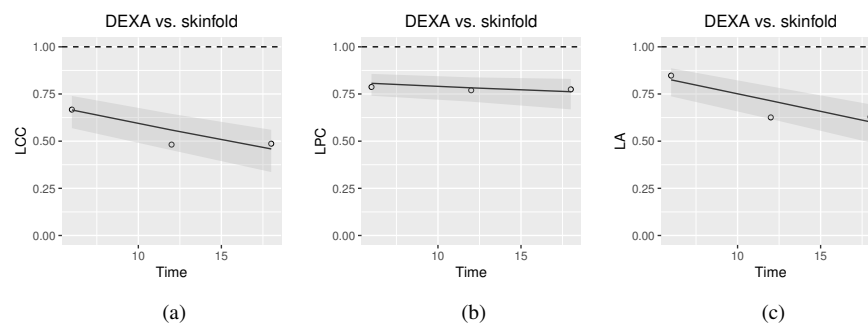


**Figure 2.** Estimate and 95% bootstrap confidence interval for the (a) longitudinal concordance correlation (LCC); (b) longitudinal Pearson correlation (LPC); and (c) longitudinal accuracy (LA) between percentage body fat measured on adolescent girls by skinfold caliper and DEXA. Points represent (a) the sample CCC, (b) sample Pearson correlation, and (c) sample accuracy.

364 Moreover, there is a moderate to weak agreement profile, where the greatest LCC estimate was 0.6654  
 365 at age 12.5 (95% CI: [0.5688, 0.7395]) and the smallest LCC estimate was 0.4588 at age 13.5 (95% CI:  
 366 [0.3354, 0.5599]). This result reinforces the discussion presented by King et al. (2007), who provided  
 367 physiological explanations for this phenomenon due to fact that the skinfold method is not capable to  
 368 detect breast, lower body and visceral fat, which increases over this age range. Clearly, as the skinfold  
 369 method detects less fat than the other, the accuracy between them tends to decrease since the expected  
 370 value difference is greater (Figure 2(c)). The concordance correlation coefficient between fitted values of  
 371 the mixed-effects model and observed values is presented as goodness of fit ( $\sigma_{\text{of}}$ ) and was approximately  
 372 0.92. This result shows that the model can reproduce the observed values quite well.

### 373 The papaya peel hue dataset

374 In commercial fruit classification, one of the most important variables is the peel hue because it is used to  
 375 determine fruit ripeness (Mendoza and Aguilera, 2004; Oliveira et al., 2017). This is very important to

376 plan harvesting procedures. In an experiment described in Oliveira et al. (2018), the hue component was  
 377 measured for a sample of 20 papaya fruits using a flat-bed scanner (HP Scanjet G2410) and a colorimeter  
 378 (Minolta CR-300) (Konica Minolta, 2003). The hue of each fruit was measured daily using both devices  
 379 for a period of 15 days, where four equidistant points on the equatorial region were observed using a  
 380 colorimeter, and 1,000 points over the same region were observed using a scanner. The circular mean  
 381 hue was calculated for the  $i$ th fruit,  $i = 1, 2, \dots, N$ , measured by the  $j$ th method,  $j = 1, 2$  at time  $t_{ik}$ ,  
 382  $k = 1, 2, \dots, n_i$ . As the multivariate von Mises distribution of the hue is highly concentrated around its  
 383 overall mean, we assume that its distribution can be treated as a normal distribution with mean  $\mu_{\bar{h}}$  and  
 384 covariance matrix  $\mathbf{R} = \mathbf{I}\sigma_{\varepsilon}^2$ .

385 The aim of the agreement study here was to determine whether the scanner can reproduce the mean  
 386 hue measurements taken by the colorimeter on the same fruit over time. The colorimeter is faster and  
 387 easier to use than a flatbed scanner. Additionally, each image obtained with the scanner needs to be processed  
 388 by an image manipulation program to select the object and extract its pixel-by-pixel information. Our  
 389 major interest here is in the longitudinal accuracy profile, because high values over time would suggest  
 390 that the fruit's topography does not influence the measurements taken by the scanner.

391 We start by making a plot of individual profiles grouped by measurement device, as well as a scatterplot  
 392 of the hue data (Figure 3). We fit a second-degree polynomial model over time for each fruit considering  
 393 all observations taken by both devices, and obtain the 95% confidence intervals for the coefficients (Figure  
 394 3(c)). Apparently, there is a moderate agreement between the scanner and the colorimeter, which increases  
 395 as the mean hue decreases. However, this could be due to the smaller number of fruits at the end of the  
 396 experiment (fruits that presented disease had to be dropped out of the study).

```
397 R> data(hue)
398 R> hue_wide <- dcast(hue, Fruit + Time ~ Method, value.var="H_mean")
399 R> p1 <- ggplot(hue_wide, aes(x = Colorimeter, y = Scanner)) +
400 +   geom_point(alpha = 0.7, colour = "black", fill = "gray", size = 1) +
401 +   geom_abline(intercept = 0, slope = 1) +
402 +   geom_smooth(se = FALSE, method = "lm")
403 R> p1 + labs(y = "Scanner", x = "Colorimeter") +
404 +   theme(legend.position = "none", aspect.ratio = 1,
405 +         axis.line.x = element_line(color="black", size = 0.5),
406 +         axis.line.y = element_line(color="black", size = 0.5))
407 R> p2 <- ggplot(hue, aes(y = H_mean, x = Time, group = Fruit)) +
408 +   facet_wrap(~ Method) + geom_line(aes(color = Fruit))
409 R> p2 + labs(y = "Mean Hue", x = "Time (Day)") +
410 +   theme(legend.position = "none", aspect.ratio = 1,
411 +         axis.line.x = element_line(color="black", size = 0.5),
412 +         axis.line.y = element_line(color="black", size = 0.5))
413 R> m.hue.1 <- lmList(H_mean ~ poly(Time, 2, raw = TRUE) | Fruit, hue)
414 R> plot(intervals(m.hue.1))
```

415 Let  $y_{ijk}$  be the peel hue measured on fruit  $i$ , using method  $j$  at time point  $k$ . We start by fitting a second  
 416 degree polynomial mixed-effects model with random intercepts, linear and quadratic coefficients, written  
 417 as

$$y_{ijk} = \beta_{0j} + b_{0i} + (\beta_{1j} + b_{1i})t_k + (\beta_{2j} + b_{2i})t_k^2 + \varepsilon_{ijk}, \quad (5)$$

$$\mathbf{b} = [b_{0i}, b_{1i}, b_{2i}]^T \sim N_3(\mathbf{0}, \mathbf{G}) \quad \text{and} \quad \varepsilon_{ijk} \sim N(0, \sigma_{\varepsilon}^2),$$

418 where  $\text{vech}(\mathbf{G}) = [\sigma_{b_0}^2, \sigma_{b_{01}}, \sigma_{b_{02}}, \sigma_{b_1}^2, \sigma_{b_{12}}, \sigma_{b_2}^2]^T$ . Under the model (5), the LCC is given by

$$\rho_{jj'}(t_k) = \frac{\mathbf{t}_k \mathbf{G} \mathbf{t}_k^T}{\mathbf{t}_k \mathbf{G} \mathbf{t}_k^T + \sigma_{\varepsilon}^2 + \frac{1}{2} S_{jj'}^2(t_k)}.$$

419 We can fit this model to estimate the LCC, LPC and LA statistics as well as to compute their 95% bootstrap  
 420 confidence intervals based on 10,000 pseudo-samples using the `lcc()` function directly:

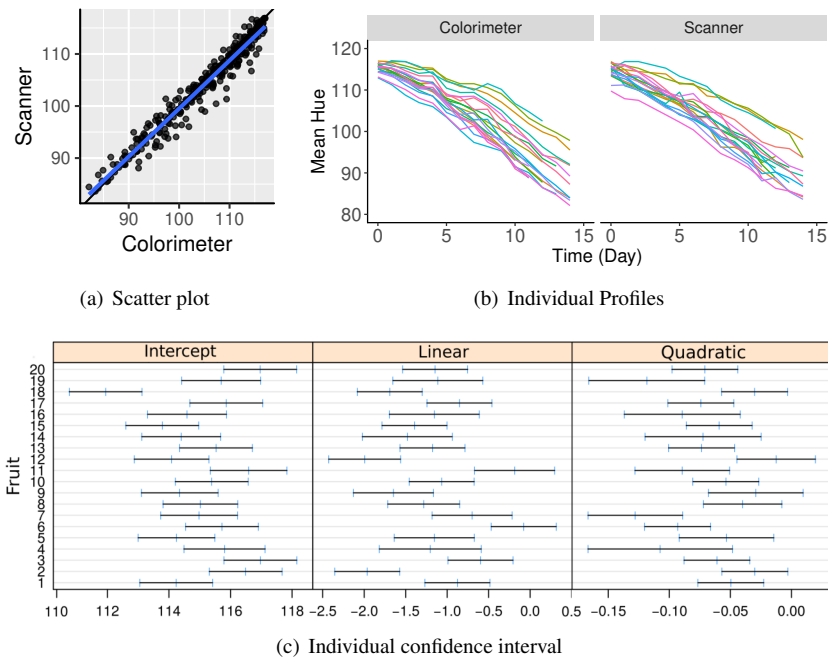


**Figure 3.** (a) Scatterplot of hue data considering all repeated measurements with a blue line representing the best fit line and the black one the line of equality, (b) Individual profiles of the peel hue of 20 papaya fruits measured by a colorimeter and a scanner, and (c) individual 95% confidence intervals for second degree polynomial coefficients fitted to the data on each fruit considering all methods together

```

421 R> m.hue.2 <- lcc(data = hue, subject = "Fruit", resp = "H_mean",
422 +               method = "Method", time = "Time", qf = 2, qr = 2,
423 +               ci = TRUE, nboot = 10000, components = TRUE)
424 Convergence error in 3074 out of 10000 bootstrap samples.

```

425 The model used to estimate  $\rho_{jj'}(t_k)$  as well as its sampled and fitted values can be extracted by  
 426 using `summary(m.hue.2, type = "model")` and `summary(m.hue.2, type = "lcc")`,  
 427 respectively. Moreover, a graphical representation of fitted values and confidence intervals for LCC, LPC  
 428 and LA can be obtained by executing

```

429 R> lccPlot(m.hue.2)
430 R> lccPlot(m.hue.2, type = "lpc")
431 R> lccPlot(m.hue.2, type = "la")

```

432 Apparently, the estimated LCC increases over time (Figure 4(a)). However, note that it is necessary to  
 433 check whether the model assumptions were fulfilled because the estimates for the LCC and its bootstrap  
 434 confidence intervals may be biased under a misspecified model. We therefore checked (i) the normality  
 435 assumption for the errors, by producing a normal plot of the within-group standardized residuals (Figure  
 436 S1(a)), which indicates that this assumption for the within-group errors is almost plausible, and is not far  
 437 from a normal distribution; ii) the homoscedasticity over time was evaluated via a plot of the standardized  
 438 residuals versus time (Figure S1(b)), which indicates an apparent residual correlation for observations  
 439 taken by the colorimeter and greater between-subject variance for observations taken by the scanner  
 440 (Figure S2); iii) the normality assumption for the random effects (Figure S1(c)), which are verified by  
 441 producing a normal plot for  $b_{0i}$ ,  $b_{1i}$  and  $b_{2i}$ . Additionally, the goodness of fit ( $gof$ ) was 0.992, indicating  
 442 a high concordance among the model fitted values and observed values. Thus, we update the model  
 443 `m.hue.2` to include different variances for each level of the factor "method", where the variance function  
 444 is given by:

$$\text{Var}(\varepsilon_{ijk}) = \sigma_{\varepsilon}^2 \delta_j^2, \text{ with } j = 1, 2.$$

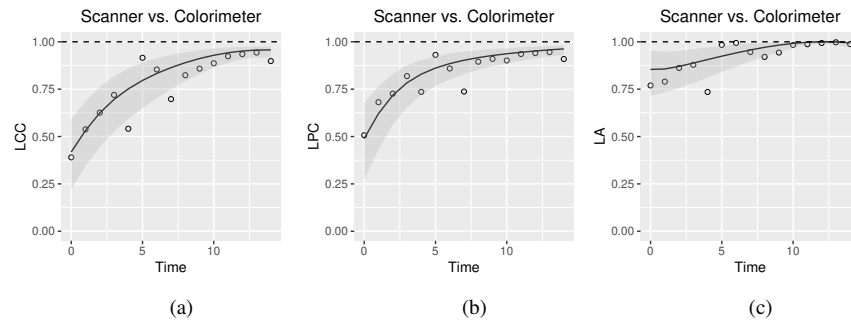


**Figure 4.** Estimate and 95% bootstrap confidence interval for the (a) longitudinal concordance correlation (LCC); (b) longitudinal Pearson correlation; and (c) longitudinal accuracy between observations measured by the scanner and the colorimeter with points that represent the (a) sample CCC, (b) sample Pearson correlation coefficient, and (c) sample accuracy, using model (5)

445 To ensure identifiability we assume that  $\delta_1 = 1$ . We also created a regular sequence from the time variable  
446 that can be used to make predictions

```
447 R> lcc_time <- with(hue, list(time = Time, from = min(Time),
448 +                           to = max(Time), n = 50))
```

449 This model can be specified in the `lcc()` as

```
450 R> m.hue.3 <- update(m.hue.2, var.class = varIdent, weights.form = "method",
451 +                   time_lcc = lcc_time,
452 +                   lme.control = lmeControl(opt = "optim"))
453 Convergence error in 981 out of 10000 bootstrap samples.
```

454 As models `m.hue.2` and `m.hue.3` are nested, we can use the likelihood ratio to test the hypothesis  
455  $H_0 : \delta_2^2 = 1$  versus  $H_a : \delta_2^2 \neq 1$ :

```
456 R> anova(m.hue.2, m.hue.3)
457 Model df      AIC      BIC    logLik    Test    L.Ratio    p-value
458 1     13    1938.125    1994.107   -956.0625
459 2     14    1934.920    1995.207   -953.4598  1 vs 2    5.205331    0.0225
```

460 The result shows that we reject  $H_0$  in favour of  $H_a$  at a significance level of  $\alpha = 0.05$ , that is, the  
461 inclusion of the function  $g(\delta_j) = \delta_j^2$  was significantly important in explaining the extra variability  
462 between observations taken at different times.

463 Moreover, the `gof` between fitted and observed values for `m.hue.3` model has, practically, the same  
464 value as presented for the `m.hue.2` model.

```
465 R> summary(m.hue.3, type = "lcc")$gof
466 [1] 0.9915905
```

467 Although the parameter  $\delta_2^2$  was important to explain the variability by method, we can see in Figure  
468 S3 that the model assumptions were still not completely fulfilled because there is a possible correlation  
469 among residuals for the colorimeter methodology. However, this model is more plausible than the first  
470 one. The sample semivariogram estimate is presented in Figure S3(b) and it appears to vary non-randomly  
471 around 0.9. Further studies involving the inclusion of correlation structures for the within-group residuals  
472 to compute the longitudinal concordance correlation function are still in development.

473 The agreement profile changes over time, being smaller at the beginning of the experiment and  
474 increasing to values close to 1 (Figure 5). If we consider values above 0.80 for the lower bound of the CI  
475 as an indication for interchangeability between the use of the two methods, the colorimeter could be used  
476 from the 12th day onwards.

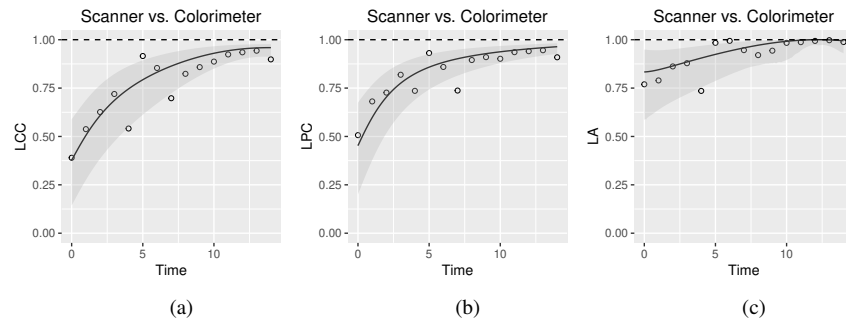


**Figure 5.** Estimate and 95% bootstrap confidence interval for the (a) longitudinal concordance correlation (LCC); (b) longitudinal Pearson correlation; and (c) longitudinal accuracy between observations measured by the scanner and the colorimeter with points that represent the (a) sample CCC, (b) sample Pearson correlation coefficient, and (c) sample accuracy, using the model that estimates different variances for each method

#### 477 **The blood draw dataset**

478 The blood draw dataset was used as an example in the `cccrm` package developed by Carrasco et al. (2013).  
 479 This dataset comes from a study conducted by the Asthma Clinical Research Network (ACRN) (Martin  
 480 et al., 2002). In this double-blinded clinical trial, 144 subjects were randomized to one of six inhaled  
 481 corticosteroid combinations, and the primary aim of the study was to estimate dose-response curves with  
 482 respect to adrenal suppression. After two weeks, the subjects were admitted for overnight testing once a  
 483 week, for the next five weeks (visits). Blood samples were collected hourly between 8pm and 8am. Then,  
 484 the plasma cortisol area under the curve (AUC) was calculated using the trapezoidal rule. A secondary  
 485 objective here was to assess the agreement of the results from blood sampling performed hourly or every  
 486 two hours, when calculating the plasma cortisol AUC. As an example, we used all individual profiles  
 487 whose expected value can be described using a second or lower degree polynomial mixed-effects model:

```
488 R> data(bdaw, package = "cccrm")
489 R> bdaw$SUBJ <- as.factor(bdaw$SUBJ)
490 R> bdaw$MET <- as.factor(bdaw$MET)
491 R> levels(bdaw$MET) <- c("1 hour", "2 hours")
492 R> length(unique(bdaw$SUBJ))
493 R> library(nlme)
494 R> fit_list <- lmList(AUC ~ poly(VNUM, 4) | SUBJ, data = bdaw)
495 R> int <- intervals(fit_list)
496 R> zero_included <- function(x) {
497 +   flag <- min(x) < 0 & max(x) > 0
498 +   return(flag)
499 + }
500 R> selected_subj <- names(
501 +   which(apply(int[, , 4], 1, zero_included) &
502 +     apply(int[, , 5], 1, zero_included)))
503 R> bdaw_subset <- subset(bdaw, SUBJ %in% selected_subj)
```

504 The scatterplot of the AUC taken every two hours as a function of the AUC taken each hour and plots of  
 505 the 19 selected individual profiles are presented in Figure 6.

```
506 R> bdaw1 <- bdaw_subset %>%
507 +   filter(MET == "1 hour")
508 R> bdaw2 <- bdaw_subset %>%
509 +   filter(MET != "1 hour")
510 R> p1 <- ggplot(bdaw_subset, aes(y = AUC, x = VNUM, group = SUBJ,
511 +   color = SUBJ)) +
512 +   geom_line(size = 0.6) + facet_wrap(~MET)
```

```

513 R> p1 +labs(y = "AUC", x = "Visits") +
514 + theme(legend.position = "none", aspect.ratio = 1,
515 + axis.line.x = element_line(color="black", size = 0.5),
516 + axis.line.y = element_line(color="black", size = 0.5))
517 R> p2 <- ggplot(bdaw1, aes(y = bdaw2$AUC, x = bdaw1$AUC)) +
518 + geom_point() +
519 + geom_smooth(method = "lm", se = FALSE) +
520 + geom_abline(intercept = 0, slope = 1)
521 R> p2 +labs(y = "AUC every 2 hours", x = "AUC every 1 hour")+
522 + theme(legend.position = "none", aspect.ratio = 1,
523 + axis.line.x = element_line(color="black", size = 0.5),
524 + axis.line.y = element_line(color="black", size = 0.5))

```

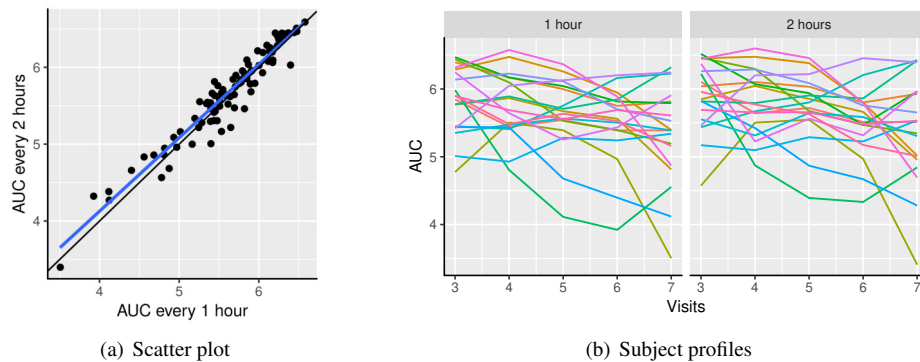


**Figure 6.** (a) Scatterplot of the blood draw data considering all repeated measurements (best fit line in blue and equality line in black), and (b) individual profiles of the plasma cortisol AUC calculated from measurements taken every hour and every two hours.

525 There seems to be a moderate to strong agreement between the plasma cortisol AUC measurements  
526 from blood draw samples taken hourly and every two hours (Figure 6(a)). Furthermore, we can also see  
527 high variability between subjects and that the AUC decreases over time for some subjects (Figure 6(b)).  
528 We begin by fitting a first degree polynomial model with a subject random intercept and slope model.

```

529 R> m.bw.1 <- lcc(data = bdaw_subset, subject = "SUBJ",
530 + resp = "AUC", method = "MET", time = "VNUM",
531 + qf = 1, qr = 1)
532 R> summary(m.bw.1, type = "lcc")$gof
533 [1] 0.8850628

```

534 This model gives only a moderate fit to the data and this is confirmed by the estimated CCC between  
535 fitted and sampled values of 0.885 (Figure 7(c)). Two possible reasons are (i) we need a higher degree  
536 polynomial mixed model to correctly describe some subject profiles, and/or (ii) a possible heteroscedasticity  
537 across time, potentially caused by three somewhat different subject profiles, that should be included in  
538 the model (7(b)). In addition, the normality assumptions for the within group error and random effects  
539 were easily checked by producing the normal plot with simulation envelope (7(e)) and seem to be broadly  
540 plausible.

```

541 R> plot(m.bw.1, which = c(1, 2, 4, 5, 6))

```

542 We now fit a second degree polynomial model with random subject effects for all coefficients and  
543 compute the 95% bootstrap confidence intervals based on 10,000 bootstrap samples for LCC, LPC and  
544 LA components.

```

545 R> m.bw.2 <- update(m.bw.1, qf = 2, qr = 2, components = TRUE,
546 + time_lcc = list(from = 3, to = 7, n = 50),

```

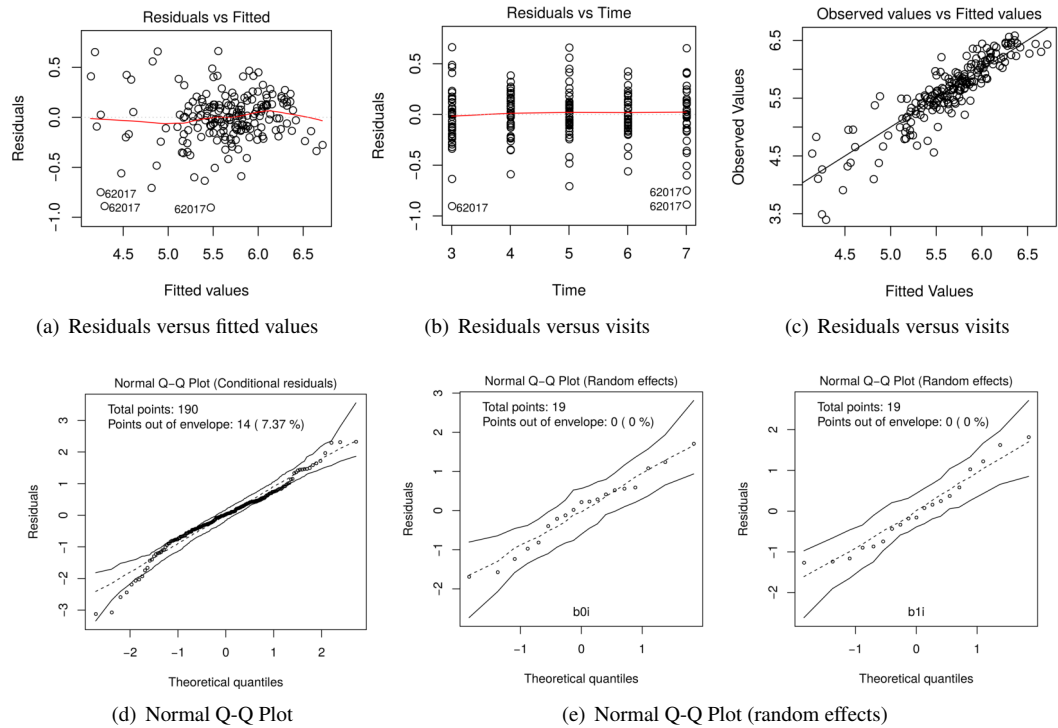


**Figure 7.** (a) plot of standardized residuals versus fitted values, (b) standardized residuals versus visits; (c) observed values versus fitted values; (d) Normal Q-Q plot with 95% simulation envelop for the conditional residuals; and (e) normal Q-Q plot with 95% simulation envelop for random effects

```

547 +             ci = TRUE, nboot = 10000, show.warnings = TRUE,
548 +             lme.control = lmeControl(msMaxIter = 200,
549 +             msMaxEval = 600, maxIter = 200))
550 Convergence error in 0 out of 10000 bootstrap samples.

```

551 The summary of the mixed effects model used to estimate LCC, LPC and LA is presented below:

```

552 R> summary(m.bw.2)
553 Linear mixed-effects model fit by REML
554 Data: Data
555 AIC          BIC          logLik
556 33.93831    75.73247    -3.969153
557
558 Random effects:
559 Formula: ~fmla.rand - 1 | subject
560 Structure: General positive-definite
561
562                                     StdDev      Corr
563 fmla.rand(Intercept)                 3.1753653 fm.(I) fd=qr=T
564 fmla.randpoly(time, degree = qr, raw = TRUE)1 1.3857944 -0.986
565 fmla.randpoly(time, degree = qr, raw = TRUE)2 0.1404521  0.961 -0.991
566 Residual                             0.1269293
567
568 Fixed effects: resp ~ fixed - 1
569                                     Value Std.Error DF t-value p-value
570 fixed(Intercept)                    6.0147  0.75167 166  8.0018  0.0000
571 fixedmethod2 hours                    0.0471  0.26203 166  0.1796  0.8576
572 fixedPoly1                          -0.0277  0.32744 166 -0.0847  0.9326

```

```

572 fixedPoly2                -0.0101  0.03315  166  -0.3046  0.7611
573 fixedmethod2 hours:Poly1  0.0107  0.11083  166  0.0967  0.9231
574 fixedmethod2 hours:Poly2 -0.0017  0.01101  166  -0.1500  0.8809
575 Correlation:
576                               fxd(I) fxdm2h fxdPl1 fxdPl2 f2h:P1
577 fixedmethod2 hours          -0.174
578 fixedPoly1                  -0.986  0.167
579 fixedPoly2                   0.961 -0.160 -0.991
580 fixedmethod2 hours:Poly1    0.172 -0.989 -0.169  0.165
581 fixedmethod2 hours:Poly2   -0.168  0.966  0.168 -0.166 -0.993
582
583 Standardized Within-Group Residuals:
584           Min           Q1           Med           Q3           Max
585 -2.97645030 -0.48398412  0.03947773  0.59922913  1.87267383
586
587 Number of Observations: 190
588 Number of Groups: 19

```

Now we can test the hypotheses

$$H_0 : \sigma_{b_0}^2 > 0, \sigma_{b_1}^2 > 0, \sigma_{b_{12}} > 0, \sigma_{b_2}^2 = \sigma_{b_{02}} = \sigma_{b_{12}} = 0 \quad \text{vs.} \quad H_a : D \text{ is positive definite}$$

589 which is equivalent to testing whether the additional variance components of the model m.bw.2 in  
590 relation to m.bw.1 are equal to zero:

```

591 R> m.bw.3 <- update(m.bw.1, qf = 2)
592 R> anova(m.bw.3, m.bw.2)
593           Model df   AIC   BIC  logLik  Test  L.Ratio  p-value
594 m.bw.3       1    10 207.642 239.792 -93.821
595 m.bw.2       2    13  33.938  75.732 -3.969 1 vs 2  179.70  <.0001

```

596 and these results clearly show that those additional variance components are important. Furthermore,  
597 the CCC between fitted and observed values also indicates that model m.bw.2 fits better than model  
598 m.bw.1, and m.bw.3.

```

599 R> summary(m.bw.1, type="lcc")$gof
600 [1] 0.8850628
601 R> summary(m.bw.2, type="lcc")$gof
602 [1] 0.9830078
603 R> summary(m.bw.3, type="lcc")$gof
604 [1] 0.8856218

```

605 Figure 5 shows the fitted LCC, LPC, and LA for concentration of plasma cortisol AUC between  
606 measurements taken every hour and taken every 2 hours and their respective 95% confidence intervals.

```

607 R> lccPlot(m.bw.2, control = list(scale_y_continuous = c(0.85, 1)))
608 R> lccPlot(m.bw.2, type = "lpc",
609 +         control = list(scale_y_continuous = c(0.85, 1)))
610 R> lccPlot(m.bw.2, type = "la",
611 +         control = list(scale_y_continuous = c(0.85, 1)))

```

612 These results show that even though the trend across time is essentially linear at the population level, there  
613 is a non-linear trend at the individual level to be more investigated. We can observe that the fitted values  
614 and confidence intervals for the LA component were very close to 1 over time, indicating a very high  
615 accuracy between methods (Figure 8(c)). Consequently, the LCC values depend almost exclusively on the  
616 LPC, which indicates a possible problem related to the precision between methods over time, suggesting  
617 the use of blood sampled every hour, rather than every two hours, is desirable for this group of patients.  
618 It is worthy to note that, as the diagnostic seems broadly plausible for the second degree mixed effects

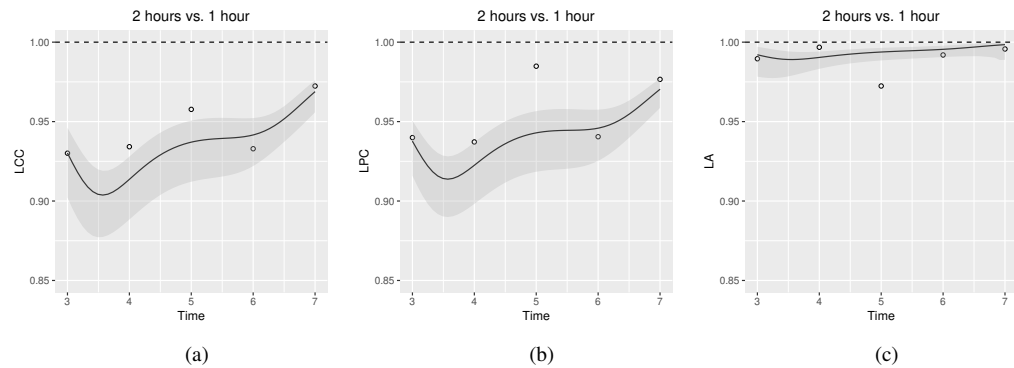


**Figure 8.** Estimate and 95% bootstrap confidence interval for (a) longitudinal concordance correlation (LCC); (b) longitudinal Pearson correlation; and (c) longitudinal accuracy for the plasma cortisol AUC between measurements taken every hour and taken every 2 hours. In addition, points that represent the sample CCC, sample Pearson correlation coefficient, and sample accuracy, respectively

619 polynomial model ( $m.bw.2$ ), under this model the LCC, LPC, and LA are fourth degree polynomials  
 620 functions of the time variable.

621 Additionally, as the `lcc()` function includes the interaction between time and method as default  
 622 through the argument `interaction = TRUE`, we can test if the interaction effect is necessary using,  
 623 for example, the following code:

```
624 R> m.bw.4 <- lcc(data = bdaw_subset, subject = "SUBJ",
625 +               resp = "AUC", method = "MET", time = "VNUM",
626 +               qf = 2, qr = 2, REML = FALSE, interaction = FALSE)
627 R> m.bw.5 <- update(m.bw.4, interaction = TRUE)
628 R> anova(m.bw.4, fit.bw5)
629      Model df   AIC   BIC   logLik   Test   L.Ratio p-value
630 m.bw.4    1   11 -2.5416 33.176 12.271
631 m.bw.5    2   13  1.2332 43.445 12.383 1 vs 2 0.22520 0.8935
```

632 As the p-value was 0.8935, we can conclude that there is no interaction effect and, consequently, the  
 633 fitted curves for each level of method over time can be considered parallel. Thus, all of these examples  
 634 show that our methodology is very flexible and can be applied to many different data types, but the  
 635 user should be careful about avoiding overfitting. We have also created a Shiny app (<https://prof-thiagooliveira.shinyapps.io/lccApp/>) using simulated data in order to stimulate people to learn more about  
 636 the LCC and verify how each parameter's value can affect the estimation of the LCC, LPC, and LA.  
 637

## 638 COMPARISON BETWEEN THE `LCC` AND `CCCRM` PACKAGES

639 In this section we review the `cccrm` R package proposed by Carrasco et al. (2013) to estimate the CCC for  
 640 repeated or non-repeated measures data and discuss how this package differs from our package `lcc`. We  
 641 can use the `ccclon()` and `ccclonw()` functions to estimate the CCC for repeated measures ( $CCC_{rm}$ )  
 642 and these were the first ones of this type available for R. Both functions estimate the CCC based on  
 643 variance components of a mixed-effects model for longitudinal data, however, the difference between  
 644 them is that `ccclonw()` uses a non-negative definite matrix of weights between different repeated  
 645 measurements (Carrasco et al., 2009).

646 These functions have been introduced to produce a value that summarizes the interchangeability  
 647 between methods in relation to all of their measurements, rather than by modeling the agreement as a  
 648 function over time (Carrasco et al., 2009). On the other hand, the `lcc()` function in package `lcc` was  
 649 developed to capture changes in the extent of the agreement profile between methods. Furthermore, the  
 650 `lcc` package also provides estimates and confidence intervals for LPC and LA that are important statistics  
 651 to make inferences on both the precision and accuracy of the measurements, respectively, and how they

652 affect the LCC at different time points, allowing the evaluation the interchangeability between methods  
653 over time.

654 We now estimate the  $CCC_{rm}$ , using package `cccrm`, between the scanner and the colorimeter  
655 measurements of the papaya peel hue dataset:

```
656 R> library(cccrm)
657 R> data(hue, package = "lcc")
658 R> ccclon(hue, "H_mean", "Fruit", "Time", "Method")
659 CCC estimated by variance components:
660      CCC      LL CI 95%      UL CI 95%      SE CCC
661 0.83767698  0.72520268  0.90660774  0.04486742
```

662 The estimate of the  $CCC_{rm}$  shows a moderate/poor agreement between the methods, suggesting  
663 that the digital image analysis of the equatorial peel region should be not used to compute the mean  
664 hue. However, suppose that the researcher had stipulated the following condition: “we would only take  
665 measurements on the equatorial region using a colorimeter if the lower band of confidence interval is  
666 greater than or equal to 0.90”. Thus, based on the lower band of the  $CCC_{rm}$  (0.725), the researcher should  
667 not use the colorimeter to compute the mean hue. On the other hand, the lower band of the LCC (Figure  
668 5) indicates that the papaya’s equatorial region can be adequately sampled through four equidistant points  
669 using a colorimeter from the ninth day. Clearly, this conclusion is only valid under the same experimental  
670 conditions.

## 671 DISCUSSION

672 The package `lcc` provides a convenient and versatile tool for estimation and inference about the LCC,  
673 LPC, and LA. The estimation of these three statistics provides a complete evaluation of the agreement  
674 between methods over time (Oliveira et al., 2018). These statistics are also very appealing for graphical  
675 illustration.

676 The package supports balanced or unbalanced (dropouts) experimental designs or observational  
677 studies, multiple methods, inclusion of covariates in the linear predictor to control systematic variation in  
678 the response, and the inclusion of different variance-covariance structures for random-effects and residuals.  
679 Residual diagnostic and goodness of fit can be evaluated easily via the generic function `plot()`, which  
680 provides up to six built-in diagnostic plots. Furthermore, the `anova()`, `AIC()`, and/or `BIC()` functions  
681 can be used to aid in model selection.

682 Statistical inference for the estimators of  $\rho_{jj'}(t_k)$ ,  $\rho_{jj'}^{(p)}(t_k)$ , and  $C_{jj'}(t_k)$  can be obtained using bootstrap  
683 confidence intervals based on approximations of their empirical distributions by the normal distribution,  
684 or from percentiles of their bootstrap sampling distribution. These methods are, however, computationally  
685 intensive.

686 To the best of our knowledge, there is no package available to estimate the extent of longitudinal  
687 agreement between methods. The `lcc` package can be viewed as an extension of the R and SAS `cccrm`  
688 package developed by Carrasco et al. (2013). This package handles the time as a factor in the model, and  
689 computes the concordance correlation coefficient, which can be viewed as a measure that summarises the  
690 interchangeability between methods in relation to all their measurements.

691 The importance in estimating the LPC, as a measure of precision, and the LA, as a measure of  
692 accuracy, was demonstrated in Section (Figure 5). In particular, both of these statistics can be used jointly  
693 to determine if a moderate or small agreement between methods at time  $t_k = t$  is related to a precision  
694 or an accuracy problem, as suggested by Lin (1989); Barnhart and Williamson (2001); Lin (1992); Ma  
695 et al. (2010). In the papaya hue example, the moderate LCC is highly influenced by a moderate LPC,  
696 suggesting that if we increase the number of points observed with the colorimeter on the equatorial region  
697 up to day 10, the colorimeter will probably be able to reproduce the measurements taken by the scanner.  
698 Future studies involve the determination of the sample size over time based on the least acceptable LCC,  
699 assuming we can accept up to a certain amount of loss in the LPC and in the LA, as discussed by Lin  
700 (1992).

701 Finally, all examples discussed in Section show that our methodology is flexible, and can be applied  
702 to many different data types. One limitation of the `lcc` package is that, for the time being, the `covar`  
703 argument only allows for including fixed-effect covariates in the linear predictor. We plan to update our

704 package in the near future to handle with the inclusion of fixed-effects and random-effects covariates, as  
705 well as interaction effects.

## 706 CONCLUSION

707 The `lcc` package implements methods to estimate the LCC, LPC and LA functions as well as their  
708 bootstrap confidence intervals. In this package, we included different structures for the variance-covariance  
709 matrices of random-effects and residuals, allowing estimation of the extent of longitudinal agreement  
710 between methods under different assumptions. Functions `plot()`, for diagnostics, `summary()` and  
711 `lccPlot()`, for numerical and graphical summaries, respectively, and `anova()`, `AIC()`, `BIC()`, for  
712 model selection, make the package flexible and easy to use. Furthermore, the mixed-effects model based  
713 approach to compute the LCC allows us to work with both balanced and unbalanced experimental designs  
714 and observational studies.

## 715 ACKNOWLEDGEMENTS

716 The authors are grateful to CNPq (National Council of Technological and Scientific Development),  
717 CAPES (Coordination for the Improvement of Higher Education Personnel), University of São Paulo, and  
718 National University of Ireland Galway, that supported this research project. We extend our thanks for  
719 the Science Foundation Ireland (SFI) under grant number SFI/12/RC/2289, co-funded by the European  
720 Regional Development Fund.

## 721 REFERENCES

- 722 Akaike, H. (1974). A New Look at the Statistical Model Identification. *IEEE Transactions on Automatic*  
723 *Control*, 19(6):716–723.
- 724 Auguie, B. and Antonov, A. (2017). `gridExtra`: Miscellaneous Functions for ‘Grid’ Graphics.
- 725 Barnhart, H. X. and Williamson, J. M. (2001). Modeling concordance correlation via GEE to evaluate  
726 reproducibility. *Biometrics*, 57(3):931–940.
- 727 Carrasco, J. L., King, T. S., and Chinchilli, V. M. (2009). The concordance correlation coefficient  
728 for repeated measures estimated by variance components. *Journal of biopharmaceutical statistics*,  
729 19(1):90–105.
- 730 Carrasco, J. L., Phillips, B. R., Puig-Martinez, J., King, T. S., and Chinchilli, V. M. (2013). Estimation of  
731 the concordance correlation coefficient for repeated measures using SAS and R. *Computer Methods*  
732 *and Programs in Biomedicine*, 109:293–304.
- 733 Chen, C. C. and Barnhart, H. X. (2013). Assessing agreement with intraclass correlation coefficient and  
734 concordance correlation coefficient for data with repeated measures. *Computational Statistics and*  
735 *Data Analysis*, 60(1):132–145.
- 736 Chinchilli, V. M., Martel, J. K., Kumanyika, S., and Lloyd, T. (1996). A Weighted Concordance  
737 Correlation Coefficient for Repeated Measurement Designs. *Biometrics*, 52(1):341–353.
- 738 Giesbrecht, F. G. and Burns, J. C. (1985). Two-Stage Analysis Based on a Mixed Model: Large-Sample  
739 Asymptotic Theory and Small-Sample Simulation Results. *International Biometric Society*, 41(2):477–  
740 486.
- 741 Harville, D. A. (1977). Maximum Likelihood Approaches to Variance Component Estimation and to  
742 Related Problems. *Journal of the American Statistical Association*, 72(358):320–338.
- 743 King, T. S. and Chinchilli, V. M. (2001). A generalized concordance correlation coefficient for continuous  
744 and categorical data. *Statistics in Medicine*, 20(14):2131–2147.
- 745 King, T. S., Chinchilli, V. M., Wang, K.-L., and Carrasco, J. L. (2007). A class of repeated measures  
746 concordance correlation coefficients. *Journal of biopharmaceutical statistics*, 17:653–672.
- 747 Konica Minolta (2003). *Precise colour communication, colour control from perception to instrumentation*.  
748 Konica Minolta Sensing.
- 749 Lin, L. I. (1989). A Concordance Correlation Coefficient to Evaluate Reproducibility. *Biometrics*,  
750 45(1):255–268.
- 751 Lin, L. I.-K. (1992). Assay Validation Using the Concordance Correlation Coefficient. *Biometrics*,  
752 48(2):599.

- 753 Lloyd, T., Chinchilli, V. M., Eggli, D. F., Rollings, N., and Kulin, H. E. (1998). Body composition  
754 development of adolescent white females. *Archives of Pediatric Adolescence Medicine*, 152:998—  
755 1002.
- 756 Loecher, M., Magrath, P., Aliotta, E., and Ennis, D. B. (2019). Time-optimized 4D phase contrast MRI  
757 with real-time convex optimization of gradient waveforms and fast excitation methods. *Magnetic  
758 Resonance in Medicine*, 82(1):213–224.
- 759 Ma, Y., Tang, W., Yu, Q., and Tu, X. M. (2010). Modeling concordance correlation coefficient for  
760 longitudinal study data. *Psychometrika*, 75(1):99–119.
- 761 Martin, R. J., Szeffler, S. J., Chinchilli, V. M., Kraft, M., Dolovich, M., Boushey, H. A., Cherniack, R. M.,  
762 Craig, T. J., Drazen, J. M., Fagan, J. K., Fahy, J. V., Fish, J. E., Ford, J. G., Israel, E., Kunselman, S. J.,  
763 Lazarus, S. C., Lemanske, R. F., Peters, S. P., and Sorkness, C. A. (2002). Systemic effect comparisons  
764 of six inhaled corticosteroid preparations. *American Journal of Respiratory and Critical Care Medicine*,  
765 165(10):1377–1383.
- 766 Mendoza, F. and Aguilera, J. M. (2004). Application of image analysis for classification of ripening  
767 bananas. *Journal of food science*, 69(9):471–477.
- 768 Moral, R. A., Hinde, J., and Demétrio, C. G. (2017). Half-normal plots and overdispersed models in R:  
769 The hnp package. *Journal of Statistical Software*, 81(10).
- 770 Oliveira, T. d. P., Hinde, J., and Zocchi, S. S. (2018). Longitudinal concordance correlation function based  
771 on variance components: an application in fruit color analysis. *Journal of Agricultural, Biological, and  
772 Environmental Statistics*, 23(2):233–254.
- 773 Oliveira, T. d. P., Zocchi, S. S., and Jacomino, A. P. (2017). Measuring color hue in “Sunrise Solo” papaya  
774 using flatbed scanner. *Revista Brasileira de Fruticultura*, 39(2):e—911.
- 775 Oliveira, T. P., Moral, R. A., Hinde, J., Zocchi, S. S., and Demétrio, C. G. B. (2019). Longitudinal  
776 Concordance Correlation.
- 777 Pandit, V., Chair, Z. B., and Schuller, B. (2019). On Many-to-Many Mapping Between Concordance  
778 Correlation Coefficient and Mean Square Error. *arXiv*, pages 1–24.
- 779 Pinheiro, J., Bates, D., Debroy, S., Sarkar, D., and core team, R. (2017). nlme: linear and nonlinear mixed  
780 effects models.
- 781 Pinheiro, J. C. and Bates, D. M. (2000). *Mixed-Effects Models in S and S-PLUS*. Springer, New York.
- 782 R core Team (2019). The R environment.
- 783 Rathnayake, L. N. and Choudhary, P. K. (2017). Semiparametric modeling and analysis of longitudinal  
784 method comparison data. *Statistics in Medicine*, 36(13):2003–2015.
- 785 Schwarz, G. (1978). Estimating the dimension of a model. In *Annals of Statistics*, pages 461–464.
- 786 Shinar, S., Berger, H., De Souza, L. R., and Ray, J. G. (2019). Difference in Visceral Adipose Tissue in  
787 Pregnancy and Postpartum and Related Changes in Maternal Insulin Resistance. *Journal of Ultrasound  
788 in Medicine*, 38(3):667–673.
- 789 Warnes, G. R., Bolker, B., Gorjanc, G., Grothendieck, G., Korosec, A., Lumley, T., MacQueen, D.,  
790 Magnusson, A., and Rogers, J. (2017). gdata: Various R Programming Tools for Data Manipulation.
- 791 Wickham, H. (2009). *ggplot2: Elegant Graphics for Data Analysis*. New York.